Precipitation Morphologies of Grain Boundary Chromium Carbides in Alloy 690TT

Yun Soo Lim, Jung Ho Han, Hai Dong Cho and Joung Soo Kim

Korea Atomic Energy Research Institute, P.O. Box 105, Yusong, Taejon 305-600, Korea

ABSTRACT

The correlation between grain boundary type characterized by coincidence site lattice (CSL) model and chromium carbide morphology in Alloy 690TT was investigated utilizing transmission electron microscopy (TEM). The chromium carbides precipitated in Alloy 690TT were identified as Cr-rich $M_{23}C_6$ by TEM analysis. The precipitation of chromium carbides was suppressed at the low angle grain boundaries with less than 15 degrees of misorientation angle between the adjoining grains. Also, carbides were seldom observed on nearly exact CSL boundaries such as Σ 11 and Σ 15, including coherent twin boundaries (Σ 3_c). On the other hand, coarse and discrete carbides were precipitated along the random high angle grain boundaries, and needle-like ones were evolved on the incoherent twin boundaries (Σ 3_i). The precipitation behaviors of chromium carbides are explained based on the grain boundary energy, which could be a variable for certain grain boundary types.

1. INTRODUCTION

In recent years, nickel-base Alloy 690 (Ni-30wt%Cr-10wt%Fe) has become a replacement material for Alloy 600 (Ni-16wt%Cr-8wt%Fe) as steam generator tubes in the nuclear power plants. Alloy 600 is well known to be very susceptible to intergranular stress corrosion cracking (IGSCC) under plant operating conditions [1]. Alloy 690, however, has been found to be immune to IGSCC in various environments [2,3]. Although no clear explanation exists for the improved IGSCC resistance in caustic and de-aerated neutral solutions, it is generally accepted that precipitation of a high density of intergranular chromium carbides by thermal treatments improves IGSCC resistance in primary water [4,5] and certain caustic environments [5,6]. Bruemmer *et al.* [7,8] suggested that the intergranular carbides promote crack tip blunting, decrease the crack tip stress state, and therefore, increase resistance to cracking.

Precipitation of second phases, such as chromium carbides, at a grain boundary is known to selectively occur. Previous studies of steels [9-13] showed that precipitation of chromium carbides is strongly influenced by grain boundary character. Singhal and Martin [10] showed that the distribution of $M_{23}C_6$ precipitates in austenitic stainless steels is quite sensitive to the degree of grain boundary misorientation. Trillo and Murr [12,13] found that, as the annealing time of 304 stainless steels increases, $M_{23}C_6$ carbides start being precipitated on the grain boundary with smaller grain boundary misorientation. Liu *et al.* [14] characterized the distribution in grain boundary character of Ni-18wt%Cr-18wt%Fe alloy with the coincidence site lattice (CSL) model, and found that the chromium carbides on the low angle grain boundary (Σ 1) and twin related grain boundaries such as Σ 9 and Σ 27 tend to be smaller and closer spaced than those of the other Σ and random high angle grain boundaries. No carbides were observed on the coherent twin boundaries (Σ 3_c), however, needle-like $M_{23}C_6$ were evolved on the incoherent twin boundaries (Σ 3_i) in their studies [9, 12-14]. All of these trends are believed to be related to the grain boundary energy, because grain boundaries with small Σ numbers usually have low energies corresponding to the energy cusps in the grain boundary energy curve [15].

The present work is an attempt to describe the correlation between grain boundary character and precipitation of intergranular chromium carbides in thermally treated Alloy 690 utilizing transmission electron microscopy (TEM). The grain boundaries were characterized according to the CSL theory [16-18], and the grain boundary types were classified into low angle, special, and random high angle (or general) grain boundaries, due to the analyzed misorientation relationships. The effects of grain boundary character on the size, density and spatial distribution of intergranular carbides were then carefully examined. Finally, the precipitation behavior of chromium carbides on the various grain boundary types was explained in terms of the grain boundary energy.

2. EXPERIMENTAL PROCEDURES

Alloy 690 tubing was obtained in the thermally treated condition (hereafter, Alloy 690TT), i.e., solution annealed at 1110 ℃ for 2 minutes, and then heat treated at 720 ℃ for 10 hours for significant growth of intergranular chromium carbides. The heat bulk composition of the major elements is given in Table 1.

Table 1. Chemical composition of Alloy 690TT (wt%)

Ni	Cr	Fe	C	N	S	Mo	Co	Mn	Al	Cu	Ti	Nb
bal.	29.6	10.5	0.02	0.017	0.001	0.01	0.01	0.32	0.02	0.01	0.26	trace

TEM specimens were prepared by cutting longitudinal strips from the tubes, grinding to flat slabs approximately 60 μm thick, and finally electropolishing the 3 mm discs. A 7 % perchloric acid + 93 % methanol solution cooled to -40 ℃ was used and a current of approximate 50 mA was applied for jet polishing. TEM examination was carried out with a JEOL 2000 FXII (operating voltage 200 kV). Specimens for optical and SEM examination were made by chemical etching with a solution of 2 % bromine + 98 % methanol. JEOL 5200 (operating voltage 25 kV) was used for scanning electron microscopy (SEM).

The grain orientation analysis was performed by Kikuchi diffraction working in a convergent beam electron diffraction mode, which results in more accurate orientation than the conventional selective area diffraction (SAD) mode. The misorientation relationship between the adjoining grains is commonly described by an angle/axis representation; the axis of misorientation, [UVW], is a direction which is common to both grains about which the first grain must be rotated by the angle of misorientation, Θ , in order to achieve the orientation of the second. In the present study, an analytic approach by Young *et al.* [19] was adopted to get the angle/axis pair. Each misorientation was represented in the form of the smallest-angle description (or, 'disorientation' representation) of the angle/axis pair.

The angle/axis pair representation of grain boundary misorientation is meaningful only if it can be used to determine the 'class' of a grain boundary, i.e., low angle, random high angle, or special with near a CSL orientation. Therefore, the next stage in the grain boundary analysis scheme is to evaluate the deviation of a particular boundary from the nearest CSL. In this study, an analytic method [20,21] based on matrix algebra was used to experimentally determine the deviation angle ($\Delta\Theta_d$) from the exact CSL orientation, The Brandon formula [16] was used as a guide to set up a significative upper limit (i.e., maximum allowable deviation angle, $\Delta\Theta_m$) for $\Delta\Theta_d$. Finally, the dislocations on some special grain boundaries were observed under the two beam conditions.

3. RESULTS

The mean linear intercept grain size excluding twins was measured to be 32 μm [22]. An optical micrograph of Fig. 1(a) reveals many annealing twins present in Alloy 690TT due to its low stacking fault energy. A twin can strongly change the precipitation behavior of intergranular chromium carbides, since an abrupt change of misorientation occurs when the twin boundary impinges on a grain boundary. The intergranular chromium carbides were significantly developed by thermal treatment on most of the grain boundaries except some special boundaries such as coherent twin boundaries (Fig. 1(b)).

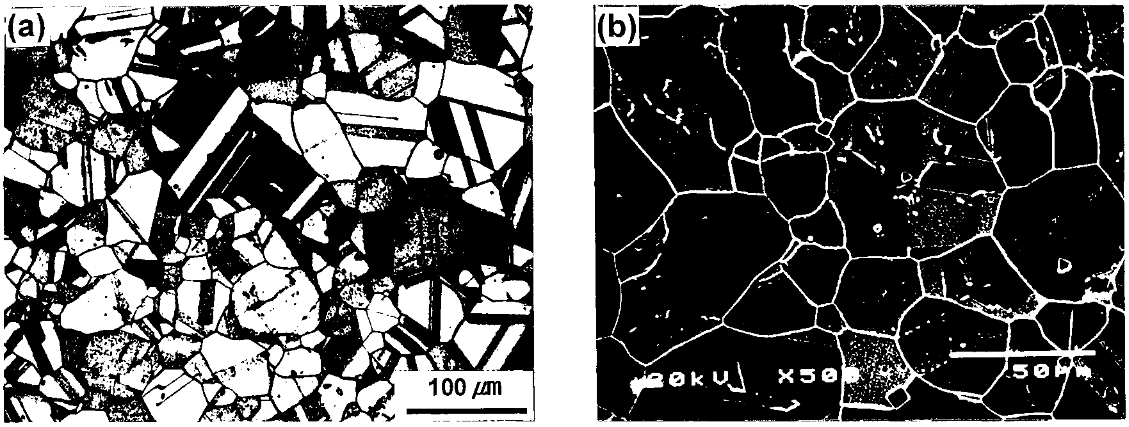

Fig.1 (a) Optical and (b) SEM micrographs of Alloy 690TT, etched in 2% bromine + 98% methanol

Fig. 2(a) is a TEM bright field image, and Fig. 2(b) is the related SAD pattern from which the intergranular chromium carbides were identified as chromium-rich (Cr-rich) $M_{23}C_6$. Cr-rich $M_{23}C_6$ has a face-centered cubic (fcc) structure, the same as Alloy 690, with a lattice constant of 1.065 nm [23], which is approximately 3 times larger than that of Alloy 690 of 0.3574 nm [24]. It is well known that Cr-rich $M_{23}C_6$ has a cube-cube orientation relationship such as $\{100\}_{\gamma}$ //$\{100\}_{M23C6}$, $<100>_{\gamma}$ //$<100>_{M23C6}$ with one grain, as shown in Fig. 2(b).

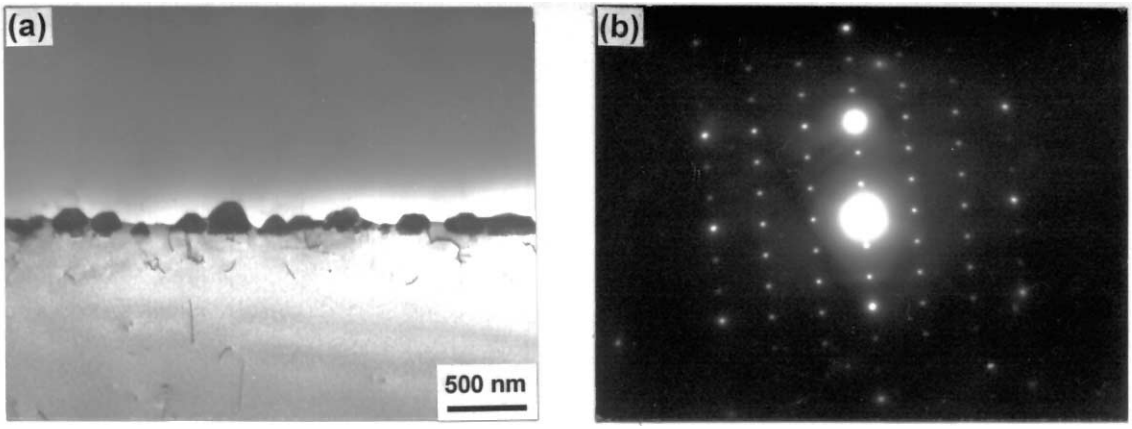

Fig. 2 (a) Grain boundary Cr-rich $M_{23}C_6$ carbides, and (b) the related SADP which shows the cube-cube orientation relationship with one grain.

In the present experiment, a low angle grain boundary was defined as one having a misorientation angle less than 15 degrees between two adjoining grains without any CSL relationship such as 12.68° /[100] of the Σ 41_a CSL boundary. The typical intergranular carbide morphology at the low angle grain boundary is shown in Fig. 3(a). The Θ /[UVW] was measured as 3.5° /[111] from the related Kikuchi diffraction patterns (Fig. 3(b)). As seen from the figure, fine and faceted carbides were densely distributed on the boundary, from which it is believed that the carbide morphology corresponds to the 'early stage of growth' after nucleation. This figure is quite different from that on the general grain boundary, on which the intergranular carbides are well developed (Fig. 2(a)). Therefore, it can be concluded that precipitation of intergranular chromium carbides is retarded on the low angle grain boundaries, compared to that on the general grain boundaries.

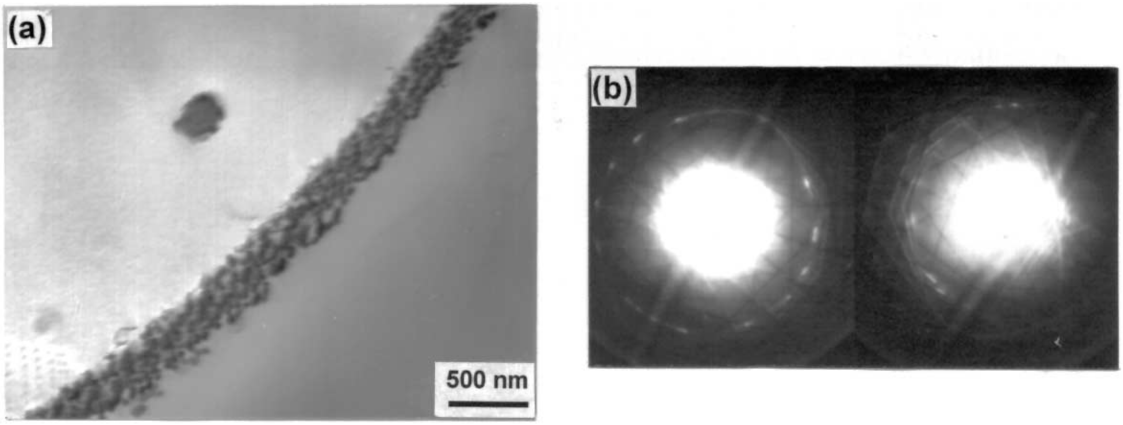

Fig. 3 (a) Low angle grain boundary with small and faceted Cr-rich $M_{23}C_6$ carbides and (b) the related Kikuchi diffraction patterns taken by a convergent electron beam.

Liu *et al.* [14] found that the portion of random high angle grain boundaries in Ni-18wt%Cr-18wt%Fe alloy was about 80 percents, discounting the contributions from Σ 3 twin boundaries and Σ 3^n (n = 2, 3, ...) twin related boundaries. Their results were in good agreement with that predicted theoretically for a random polycrystalline aggregate [25]. The grain boundaries in Fig. 4 were interpreted as random high angle, because the misorientation angles were above 15 degrees without having any precise CSL misorientations up to Σ 49 within the limit of the maximum allowable deviations given by the Brandon criterion. As shown in the figures, coarse and irregular carbides were discretely distributed on the grain boundaries, and these are the ones commonly found in thermally treated Alloy 690. In Fig. 4(a), some faceted carbides appeared to be combined each other, to form a large irregular shape. Therefore, the time development of precipitation of intergranular carbides on these grain boundaries corresponds to the 'stage of concurrent coalescence and growth'. This feature is quite different from the case of the low angle grain boundary, on which the precipitation of carbides was only at the early stage of growth in spite of the same heat treatment conditions.

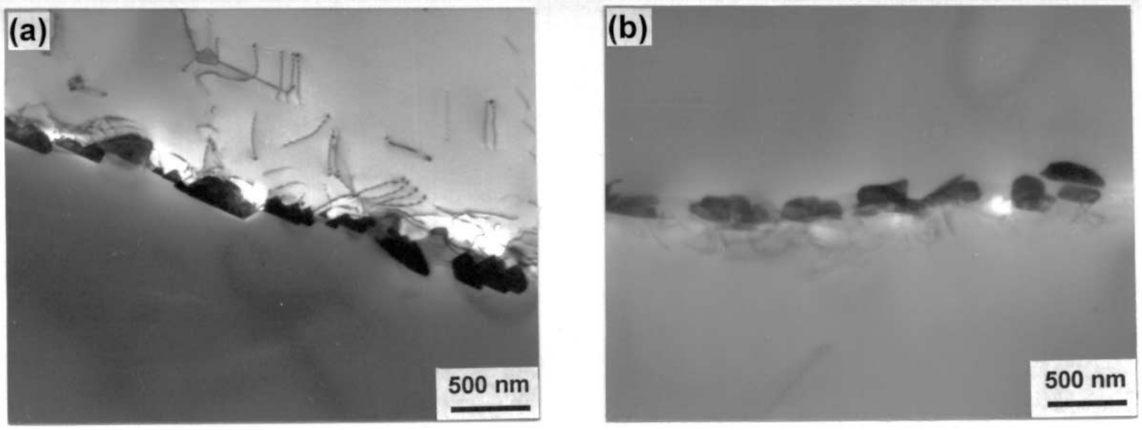

Fig. 4 Random high angle grain boundaries with coarse and discrete Cr-rich $M_{23}C_6$ on the boundaries.

Some CSL boundaries with Σ 3_c , Σ 11 and Σ 15 are shown in Fig. 5. The experimental deviations of the boundaries from the precise CSL misorientation were much smaller than the ones calculated by the Brandon formula. Therefore, they were well classified as the CSL boundaries. The carbide morphologies shown in the figures were typically found on the CSL boundaries in the alloy. Firstly, most of the coherent twin boundaries (Σ 3_c) were found to have the negligible deviation from the precise Σ 3 CSL misorientation, and the carbide was never found on the boundaries under the present experimental conditions (Fig. 5(a)). Secondly, they were not precipitated, the same as on the coherent twin boundary (Fig. 5(b)), or tiny ones were densely distributed, similar to the case of the low angle grain boundary (Fig. 5(c)). Therefore, it can be concluded that the precipitation of intergranular carbides is suppressed on the CSL boundaries, as compared to the case of the general grain boundaries.

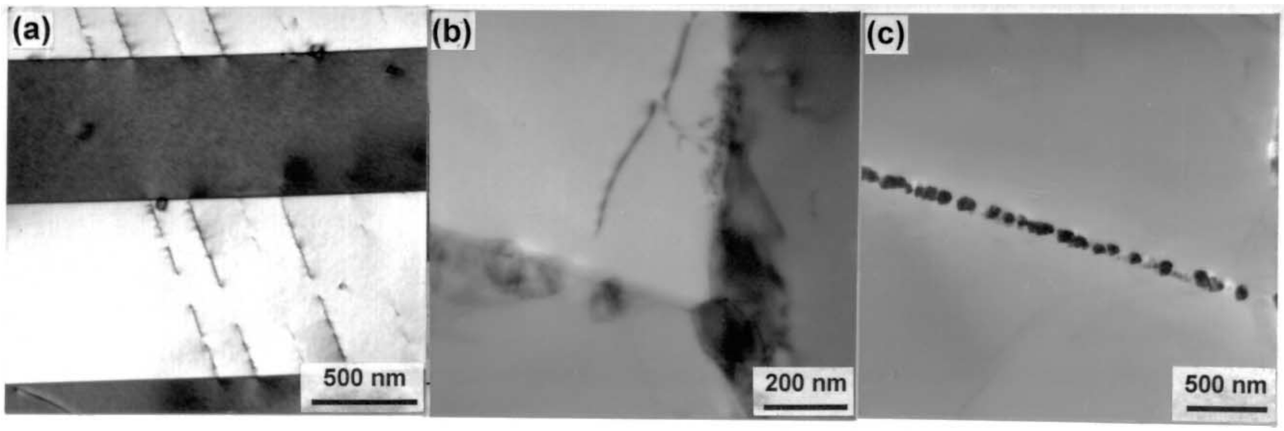

Fig. 5 Some CSL boundaries with Σ values of (a) 3_c, (b) 15, and (c) 11. The precipitation of grain boundary Cr-rich $M_{23}C_6$ was suppressed on these boundaries.

On the other hand, needle-like carbides were precipitated on the incoherent twin boundaries ($\Sigma\ 3_i$), as shown in Fig. 6(a). They appeared to grow parallel to the coherent twin boundary, as reported [9,26]. It was confirmed from the SAD patterns that the carbides, Cr-rich $M_{23}C_6$, also have the cube-cube orientation relationship with the matrix, same as in the case of the intergranular carbides. The difference in carbide precipitation on the coherent and incoherent twin boundaries (Fig. 5(a), Fig. 6(a)) demonstrates the importance of the orientation of the grain boundary plane itself, in addition to the misorientation/axis description, for the precipitation of intergranular carbides. The coherent twin boundary is parallel to the {111} twining plane, and the atoms in the boundary fit perfectly into both grains. Therefore, the atoms in the boundary are essentially in undistorted positions, resulting in the extremely low energy in comparison with the energy of a random high angle grain boundary. However, the incoherent twin boundary does not lie exactly parallel to the twining plane, and the atoms do not fit perfectly into each grain. Therefore, the boundary energy is much higher than the energy of the coherent twin boundary, even though it is still much lower than that of the random high angle grain boundary. In the alloy, other intragranular carbides were not observed under the present heat treatment conditions.

Discontinuous precipitates are commonly found in nickel-base alloys [3,26], as shown in Fig. 6(b). It is well known that discontinuous precipitation is associated with the concurrent grain boundary migration, and is largely dependent on the grain boundary energy, mobility and diffusivity, which depend in turn on the grain boundary structure [27]. Therefore, it is considered that discontinuous precipitation can be preferentially initiated on the grain boundaries with a particular misorientation relationship and grain boundary structure [28]. In addition, Fig. 6(b) illustrates how the twin boundary (denoted 'TB') influences intergranular precipitation. The intergranular carbides were discontinuously precipitated in the cellular form on the grain boundary enclosed by the twin, however, particulate precipitates were evolved on the other part of the same grain boundaries. From the above results, it can be concluded that interception by twins may result in large changes in misorientation and hence in the structure of the parent boundary, from which drastic changes in precipitation behavior of intergranular carbides are expected.

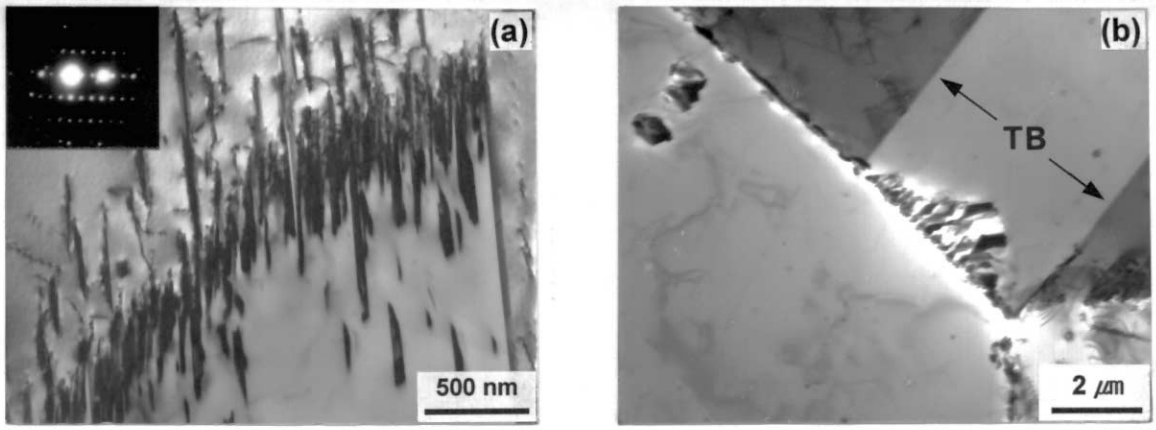

Fig. 6 (a) Needle-type Cr-rich $M_{23}C_6$ on the incoherent twin boundary having a cube-cube orientation relationship with the matrix, and (b) typical discontinuous precipitates of Cr-rich $M_{23}C_6$ in thermally treated Alloy 690. The twin boundaries are denoted TB in (b).

The CSL model is based upon the assumption that the grain boundary energy can be extremely low if there is atomic regularity on that boundary.

4. DISCUSSION

When classifying a grain boundary using the CSL model, it is quite important to correctly estimate its deviation from a precise CSL misorientation and to determine if it comes under the category of a CSL boundary. Fixing the maximum allowable deviation from the exact CSL misorientations which may be admitted for the criteria of specialness is also equally important, but has been far from well established. Several contradictory results were reported on this subject [21,29,30]. For example, Martikainen and Lindroos [29,30] found agreement between the secondary grain boundary dislocation models and the observed periodicity on the boundary in spite of the larger misorientation than that given by the Brandon criterion. This fact indicates the possibility of accommodating misorientation from certain coincidence orientation relationship to larger secondary rotations than previously assumed.

In the present study, it was found that 1) intergranular chromium carbide was never precipitated on the coherent twin boundaries ($\Sigma\ 3_c$), however, needle-like ones were evolved on the incoherent twin boundaries ($\Sigma\ 3_i$), 2) precipitation was retarded on the low angle grain boundaries (Σ 1) and well-defined CSL boundaries (Σ 11, Σ 15, etc.), 3) on the other hand, carbides were significantly developed on the random high angle grain boundaries. These results were in agreement with the previous studies [9,12-14,24,26].

The above results can be understood, in part, in terms of the influence of grain boundary energy. The extremely low energy of coherent twin boundary in a nickel-base alloy [31] could be a reason for the absence of intergranular carbides on the boundary. Similarly, their suppression on the low angle and CSL boundaries, in comparison with that on the random boundaries, could also be attributed to the difference in their grain boundary energies. It is well known that the grain boundary energy increases in a linear manner as misorientation increases up to 10 - 15° , and after this stage the grain boundary energy is almost independent of misorientation, with the energy cusps at given CSL misorientations [15]. The changes of grain boundary energy could, therefore, be responsible for the observed intergranular carbide morphology on the various types of grain boundaries.

5. CONCLUSIONS

1. Many annealing twins were present in the thermally treated Alloy 690 due to its low stacking fault energy. The intergranular carbides were significantly developed along most of the grain boundaries. The carbides precipitated on the grain boundaries were identified as Cr-rich $M_{23}C_6$, and found to have a cube-cube orientation relationship such as $\{100\}_\gamma$ //$\{100\}_{M23C6}$, $<100>_\gamma$ //$<100>_{M23C6}$ with one grain.

2. The grain boundaries with coarse and discrete carbides were characterized as random high angle (or general). On the other hand, fine and faceted carbides were densely distributed on the low angle grain boundaries. On the CSL boundaries established by the Brandon criterion, carbides were hardly precipitated or their morphology was similar to the case of low angle grain boundaries. Therefore, it could be concluded that the precipitation of intergranular carbides is retarded (or suppressed) on low angle and CSL boundaries, in comparison with that on random high angle grain boundaries. The precipitation behavior of intergranular carbides could be, in part, explained by the influence of grain boundary energy.

ACKNOWLEDGMENTS

This work has been carried out as a part of the Steam Generator Materials Project under the Nuclear R&D Program sponsored by MOST in Korea.

REFERENCES

1. Marston, T.U. and Jones, R.L., "Materials Degradation Problems in the Advanced Light Water Reactors", *Proc. of the Fifth International Symposium on Environmental Degradation of Materials in Nuclear Power Systems – Water Reactors*, pp. 3-9, American Nuclear Society, La Grange Park, Il, August 1991.
2. Page, R.A., "Stress Corrosion Cracking of Alloys 600 and 690 and Nos. 82 and 182 Weld Metals in High Temperature Water", *Corrosion*, Vol. 39, 1983, pp. 409-421.
3. Payne, S.M. and McIntyre, P., "Influence of Grain Boundary Microstructure on the Susceptibility of Alloy 600 to Intergranular Attack and Stress Corrosion Cracking", *Corrosion*, Vol. 44, 1988, pp. 314-319.
4. De, P.K. and Ghosal, S.K., "A Comparative Study of Stress Corrosion Cracking of Steam Generator Tube Materials in Water at 315C", *Corrosion*, Vol. 37, 1981, pp. 341-349.
5. Airey, G.P., "Optimization of Metallurgical Variables to Improve Corrosion Resistance of Inconel Alloy 600", EPRI Report No. NP-3051, July 1983.
6. Cels, J.R., "Caustic Stress Corrosion Cracking Studies at 288 C (550 F) Using the Straining Electrode Technique – Comparison of Alloy 600, Alloy 800, and Type 304 Stainless Steel", *Corrosion*, Vol. 34, 1978, pp. 198-209.
7. Bruemmer, S.M. and Henager, Jr. C.H., "High Voltage Electron Microscopy Observations of Microdeformation in Alloy 600 Tubing", *Scripta Metall.*, Vol. 20, 1986, pp. 909-914.
8. Bruemmer, S.M., Charlot, L.A. and Henager, Jr. C.H., "Microstructure and Microdeformation Effects on IGSCC of Alloy 600 Steam Generator Tubing", *Corrosion*, Vol. 44, 1988, pp. 782-788.
9. Lewis, M.H. and Hattersley, B, "Precipitation of $M_{23}C_6$ in Austenitic Steels", *Acta Metall.*, Vol. 13, 1965, pp. 1159-1168.
10. Singhal, L.K. and Martin, J.W., "The Growth of $M_{23}C_6$ Carbide on Grain Boundaries in an Austenitic Stainless Steel", *Trans. Metall. Soc. AIME*, Vol. 242, 1968, pp. 814-819.
11. Lartigue, S. and Priester, L., "Stability of Extrinsic Grain Boundary Dislocations in Relation with Intergranular Segregation and Precipitation", *Acta Metall.*, Vol. 31, 1983, pp. 1809-1819.

12. Trillo, E.A. and Murr, L.E., "A TEM Investigation of $M_{23}C_6$ Carbide Precipitation Behavior on Varying Grain Boundary Misorientations in 304 Stainless Steels", *J. Mater. Sci.*, Vol. 33, 1998, pp. 1263-1271.
13. Trillo, E.A. and Murr, L.E., "Effects of Carbon Content, Deformation, and Interfacial Energetics on Carbide Precipitation and Corrosion Sensitization in 304 Stainless Steel", *Acta Mater.*, Vol. 47, 1999, pp. 235-245.
14. Liu, H., Gao, M., Harlow, D.G. and Wei, R.P., "Grain Boundary Character, and Carbide Size and Spatial Distribution in a Ternary Nickel Alloy", *Scripta Metall. Mater.*, Vol. 32, 1995, pp. 1807-1812.
15. Balluffi, R.W., "Grain Boundary Diffusion Mechanisms in Metals", *Metall. Trans. A.*, Vol. 13A, 1982, pp. 2069-2094.
16. Brandon, D.G., "The Structure of High-Angle Grain Boundaries", *Acta Metall.*, Vol. 14, 1966, pp. 1479-1484.
17. Grimmer. H., Bollmann, W. and Warrington, D.H., "Coincidence-Site Lattices and Complete Pattern-Shift Lattices in Cubic Crystals", *Acta Cryst.*, Vol. A30, 1974, pp. 197-207.
18. Smith, D.A. and Pond, R.C., "Bollmann's 0-Lattice Theory; A Geometrical Approach to Interface Structure", *Int. Met. Rev.*, Vol. 21, 1976, pp. 61-74.
19. Young, C.T., Steele Jr., J.H., and Lytton, J.L., "Characterization of Bicrystals Using KiKuchi Patterns", *Metall. Trans.*, Vol. 4, 1973, pp. 2081-2089.
20. Bleris, G.L., Antonopoulos, J.G., Karakostas, Th. and Delavignette, P., "Grain Boundary Analysis in TEM", *Phys. Stat. Sol. (a)*, Vol. 67, 1981, pp. 249-257.
21. Dechamps, M, Baribier, F. and Marrouche, A., "Grain Boundaries: Criteria of Specialness and Deviation from CSL Misorientation", *Acta Metall.*, Vol. 35, 1987, pp. 101-107.
22. ASTM E112-88, "Standard Method for Determining Average Grain Size", Vol. 03.01, pp. 294-319, ASTM, Philadelphia, 1992.
23. Bowman, A.L., Arnold, G.P., Storms, E.K. and Nereson, N.G., "The Crystal Structure of $Cr_{23}C_6$", *Acta Cryst.*, Vol. B28, 1972, pp. 3102-3103.
24. Lee, Y.B., Jang, J.S., Lee, D.H., Lee, D.Y. and Kuk, I.H., "Selective Precipitation of Carbides in Alloy 690", *J. Kor. Inst. Met. & Mater.*, Vol. 35, 1997, pp. 935-941.
25. Morawiec, A., Szpunar, J.A. and Hinz, D.C., "Texture Influence on the Frequency of Occurrence of CSL-Boundaries in Polycrystalline Materials", *Acta Metall. Mater.*, Vol. 41, 1993, pp. 2825-2832.
26. Angeliu, T.M. and Was, G.S., "Behavior of Grain Boundary Chemistry and Precipitates upon Thermal Treatment of Controlled Purity Alloy 690", *Metall. Trans. A*, Vol. 21A, 1990, pp. 2097-2107.
27. Gottstein, G. and Schwarzer, F., "On the Orientation Dependence of Grain Boundary Energy and Mobility", *Mater. Sci. Forum*, Vol. 94-96, 1992, pp. 187-207.
28. Hirth, S. and Gottstein, G., "Misorientation Effects on Discontinuous Precipitation in Al-Ag-Ga", *Acta Metall.*, Vol. 46, 1998, pp. 3975-
29. Martikainen, H.O. and Lindroos, V.K., "Grain Boundary Structure far from High Density Coincidence Site Lattice Orientation Relationship in Ferritic Stainless Steel", *Acta Metall.*, Vol. 31, 1983, pp. 1909-1917.
30. Martikainen, H.O. and Lindroos, V.K., "grain Boundary Structural Changes during Annealing and High Temperature Deformation of Ferritic Stainless Steel", *Acta Metall.*, Vol. 33, 1985, pp. 1223-1234.
31. Murr, L.E., "Interfacial Free Energy", Chapter 3, *Interfacial Phenomena in Metals and Alloys*, Addison-Wesley, Reading, Mass., 1975.